Mining of Mineral Deposits
Volume 17 (2023), Issue 1, 108-119

https://doi.org/10.33271/mining17.01.108

An approach based on Machine Learning Algorithms, Geostatistical Technique, and GIS analysis to estimate phosphate ore grade at the Abu Tartur Mine, Western Desert, Egypt

Abdelrahem Embaby[1], Ashraf Ismael[1], Faisal A. Ali[1], H.A. Farag[1], B.G. Mousa[1*], Sayed Gomaa[1], Mohamed Elwageeh[2]

[1] *Department of Mining and Petroleum Engineering, Faculty of Engineering, Al-Azhar University, Cairo, Egypt*
[2] *Mining, Petroleum, and Metallurgical Engineering Department Cairo University, Giza, Egypt*

**Corresponding author: e-mail dr.bahaa1@azhar.edu.eg*

Abstract

Purpose. This paper aims to estimate phosphate ore grade in the Abu Tartur area, Western Desert, Egypt, using four Machine Learning Algorithms (MLA), Geostatistical Techniques (variogram and kriging models), and GIS-analysis.

Methods. Four machine-learning techniques include Optimizable Decision Tree (ODT), Optimizable Support Vector Machine (OSVM), Optimizable Gaussian Process Regression (OGPR), Artificial Neural Network (ANN) are applied in this paper. The constructed variogram and kriging models, as well as GIS-analysis, provide a clear understanding of all the elements distributed in the Abu Tartur phosphate ore and are very useful at the planning and mining stages.

Findings. Phosphate content has been estimated with high accuracy based on the results of four machine-learning techniques. The most efficient technique for estimating phosphate content is optimizable (OGPR), which gives correlation coefficients (R) of 0.933 and 0.927 with Mean Absolute Errors (MAE) of 0.983 and 0.933 for the training and validation data, respectively. In addition, geostatistical and GIS methods have shown that percentage of P_2O_5, thickness, and Fe% are suitable for phosphate mining processes, except for small pockets that require little attention at the mining stage.

Originality. This research attempts to develop a quick estimation of phosphate ore grade and to provide a clear understanding about the distribution of different constituents within the ore body using different techniques.

Practical implications. Grade estimation is commonly reduced to a function approximation. Artificial intelligence (AI) techniques, and in particular the chosen type of AI techniques, can provide, a valid methodology for estimating grade, and the proposed models can be applied to any other data in the range used in this research.

Keywords: *Machine Learning Algorithms (MLA), geostatistical and GIS modeling, Abu Tartur phosphate ore*

1. Introduction

Artificial neural networks (ANNs) are the result of decades of research into the biologically motivated computing paradigm. There are many different opinions about their definition and applicability to technological problems. However, it is widely believed that ANNs represent an alternative to the concept of programmed or hard computing. The ever-emerging ANN technology has brought the concept of neural computing, which is increasingly used in real engineering problems. ANNs Introduction 19 are parallel computing structures, which replace program development with learning [1]-[6]. In the past, there have been many cases of successful application of ANNs to problems of function approximation, prediction, and pattern recognition. This fact, as well as the special characteristics of ANNs, makes them a natural choice for estimating the phosphate ore grade issues. As discussed in the previous paragraphs, grade estimation is commonly reduced to a function approximation. The ANNs, and in particular the chosen type of ANNs, can provide a valid methodology for grade estimation. Therefore, many researchers have used Machine Learning Algorithms.

Geostatistical and GIS modeling is used as a new method for calculating and predicting the ore grade [7]-[20]. B. Samanta et al. [7] evaluate several global and local learning methods for evaluating the ore grade in three deposits: iron ore, gold and bauxite, using artificial neural networks. For this, four local learning algorithms have been studied: quick prop back-propagation, back-propagation with momentum, standard back-propagation, and Levenberg-Marquardt back-propagation, as well as two global learning algorithms – NOVEL and simulated annealing. The study findings show that the use of global learning algorithms instead of local learning algorithms does not provide any advantages. The similar performance of global and local learning algorithms is caused by the smooth error surface of neural network training for these specific case studies. A separate experiment that compares the performance of global and local learning algorithms for a nonlinear multimodal optimization of a Rastrigin function

Received: 24 September 2022. Accepted: 12 March 2023. Available online: 30 March 2023

Mining of Mineral Deposits. ISSN 2415-3443 (Online) | ISSN 2415-3435 (Print)

consisting of several local minima unmistakably shows that global learning approaches are superior to local learning algorithms. Even though the use of global learning methods in neural network training for these specific case studies has not been beneficial, it is nevertheless desirable to do so, since many real-world applications of neural network modeling have problems with local minima on the error surface.

Jalloh Abu Bakarr et al. [8] proposed to combine Artificial Neural Networks with Geostatistics for the best assessment of mineral reserves. The definition of ANNMG is an artificial neural network model related to geostatistics. The Artificial Neural Network has been trained, tested and confirmed using analysis data obtained from exploration drill holes. The validated model was then used to generalize the mineral grades from known and unknown sampling locations within the drilling zone. The reproduced and generalized analysis data were combined and sent to geostatistics to construct a geological 3D block model. The regression analysis findings have revealed a striking similarity between the expected and actual sample grades. The ANNMG generalized grades show that this method can be used to augment exploratory efforts and reduce costs.

Shaofu He and Fei Li [9] use the traditional classification analysis strategy: compensation samples were obtained using neural network analysis and database analysis, an artificial network model was built, and the procedure was simplified. A neural network model has also been developed. A new network model was used to study the geographic information systems of counties A and B. In county A, 61 geological disasters have been revealed, of which 4 collapses, 47 landslides, and 10 unstable slopes. In county B, there are 19 natural disasters, including 6 landslides, 4 collapses, and 9 unstable slopes. In terms of geographic prediction combined with the network model, the comparison with the actual situation reveals that the geographical distribution is less in the non-prone areas, with a proportion of 0.3%, and is 99.7% in the areas vulnerable to geological and geographic disasters. The percentage of low points affected by geological disasters is 76.9%, while the percentage of low disaster-affected points is 22.8%. The division of geographical and geological classes by the assessment model is essentially consistent with the real grades, which can satisfy the requirements of the geographic assessment. In essence, it is understood that a more thorough and useful artificial neural network model is created starting with the geographic information system of the model.

According to B.C. Sarkar and others [10], in one type of Banded Iron Formation (BIF) of an iron ore deposit in East India, an attempt was made to estimate the distribution of iron ore grade using geostatistics and ANN-based models. According to geology, supergene iron ore is created by enriching the parent material (BIFs) through the progressive leaching of impurities like SiO_2 and Al_2O_3. The distribution of Fe varies depending on regional factors that influence on the ore formation, because the degree of leaching varies by region. The ANN models a non-linear distribution and is often used as a global approximator, whereas geostatistical approaches are based on models in terms of regional correlations of mineralization characteristics. Using ordinary kriging (OK) and sequential Gaussian simulation (SGS), the spatial distribution modeling of Fe values has been done. Hybrid Neural Networks (HNN) is used in non-linear modeling to provide an alternative method for estimating the grade. Using conventional statistical modeling, a negative 3-parameter lognormal Fe population with a mean of 60.49%, skewness of -0.08, and kurtosis of 2.60 has been determined.

Block-by-block kriging estimates with associated kriging variance were derived as a result of semi-variography and geostatistical estimation using the OK approach. This resulted in an overall mean kriging estimate and kriging variance of Fe of 60.29% and 7.76% 2, respectively. The SGS method results show that the average value of Fe is 60.71% with a standard deviation of 5.89% and minimum and maximum values of 45.12% and 68.70%, respectively. The Mean Squared Error (MSE) and correlation coefficient (R^2) values for the HNN model were 12.33 and 0.61, respectively, indicating the model's ability to withstand the greatest heterogeneity within the target domain. Comparing Fe grade estimations from kriging, simulation and HNN models reveals that they more or less retain distribution patterns similar to the sample data. It is suggested that in order to create alternate scenarios for improving mine planning and design activities, grade prediction should be conducted using all three modeling methodologies. The methods provide the basis for convincing grade modeling, which leads to more advanced methods for estimating iron ore reserves.

The mining sector primarily uses traditional geostatistical approaches to estimate ore reserves. The geological complexity of mining ore bodies makes the determination of mineral reserves an important task for mining engineers. Numerous advanced predictive spatial mapping techniques have been developed over the years as a result of extensive research; these techniques can be used to estimate ore reserves. More recently, advances in the application of Machine Learning Algorithms (MLA) have offered a new method for solving the problem of ore reserve estimation. A complex drill-hole dataset that demonstrates the typical scatter and inaccuracies that can be associated with a mining dataset is used to elaborate on the application of MLA and the numerous problems associated with their use for reserve estimation. The generalization capabilities of NN and Support Vector Machines (SVM) are compared with the geostatistical ordinary kriging (OK) approach to test the accuracy and applicability of MLA for mineral resource estimation [11].

To predict the grade distribution within a mineral deposit, Umit Emrah Kaplan and Erkan Topal [12] proposed a grade estimation technique that combines multilayer feed-forward neural network (NN) and k-nearest neighbor (kNN) models. The geological data (lithology and alteration) and sample locations (east, north and altitude) obtained from the drill-hole data are used to develop the models. The proposed method provides the identification of patterns according to the data of chemical composition (mineral grade) and geological aspects. The kNN method is used to forecast rock types and their modifications in unsampled areas prior to grade estimation. In contrast to the conventional model that uses only the coordinates of the sample points as input, the case study presented here shows that the proposed approach has a mean absolute error (MAE) of 0.507 and $R^2 = 0.528$, while the conventional model has an MAE value of 0.862 and $R^2 = 0.112$. The proposed method appears promising and may offer an alternative method for estimating grades in comparable modeling projects.

The performance of four Machine Learning Algorithms (MLA) – Artificial Neural Network (ANN), Support Vector Machine (SVM), Decision Tree (DT), and Random Forest – for forecasting daily energy consumption is compared in a

comparative Study of Energy Consumption Forecasting Algorithms for an Experimental Open-Pit Mine (RF). The models were developed, tested and then assessed. Four metrics – R, MAE, root mean squared error (RMSE), and root relative squared error – were used in the study to evaluate the performance of the models (RRSE). The results show that RF is the most accurate predictive model for energy forecasting [13].

To estimate significantly skewed data for gold in the Quartz Ridge vein type, Zaki et al. [14] used five Machine Learning Algorithms, including Decision Tree Ensemble (DTE), Gaussian Process Regression (GPR), Fully Connected Neural Network (FCNN), Support Vector Regression (SVR), and K-Nearest Neighbors (K-NN). The accuracy of MLA differs from that of geostatistical techniques such as ordinary and indicator kriging. Data pre-processing and separation have been significantly improved resulting in an accurate MLA estimation. To improve the network training performance and reduce significant variances in the ranges of the dataset variables for predictions, the data were pre-processed using two normalization approaches (z-score and logarithmic). Using an integrated data segmentation method based on the Marine Predators Algorithm, the samples were divided into two equal sections (MPA). The ranking demonstrates that the GPR with logarithmic normalization is superior to kriging approaches and is the most effective method for estimating gold grade.

One of the important minerals needed for plant growth is phosphorus. Although it is relatively available in nature, most soils, especially calcareous soils, lack this component. The cheapest source of phosphorus fertilizer is phosphate rock, which can come from either igneous or sedimentary sources [21].

Phosphate rocks have been found in Egypt since the turn of the century, and between 1908 and 1911, foreign corporations began to mine them in the Kharga Oases of the Western Desert and other areas near the Red Sea and Nile Valley. Since then, phosphate mining and production have continued to this day in the first two zones. Three facies belts can be used to classify phosphate rock occurrence in Egypt (Fig. 1).

Figure 1. Egyptian Phosphate belt

The Nile Valley between Qena and Idfu, especially near Sebaiya and El Mahammid, in Gabel Abu Had and Wadi Qena, which have larger industrial deposits, and the Western Desert on the Abu Tartour plateau between the Dakhla and Kharga oases are the only places where the economy is restricted and concentrated [22]. Therefore the aim of this study is to estimate the grade of the Abu Tartour phosphate ore mine in the Western Desert of Egypt using four Machine Learning techniques: an Optimizable Decision Tree (ODT), an Optimizable Support Vector Machine (OSVM), an Optimizable Gaussian Process Regression (OGPR), and an Artificial Neural Network (ANN) in addition to geostatistical and GIS modeling.

1.1. Discerption and geological setting of the study area

The Abu Tartour plateau is located 50 km west of the city of El Kharga (the capital of New Valley governorate in southwestern Egypt) and 10 km from the main road between the EI-Kharga and EI-Dakhla Oases, 300 km from the city of Asyut on the Nile River and 650 km from Cairo. The Abu Tartour plateau is located in the Kharga-Dakhla region, extending from the Kharga Oasis westwards to the Dakhla oasis. The length is about 150 km from north to south between latitudes 24°15′ and 26°05′N, and about 275 km from west to east between longitudes 27°50′ and 30°55′E (Fig. 2).

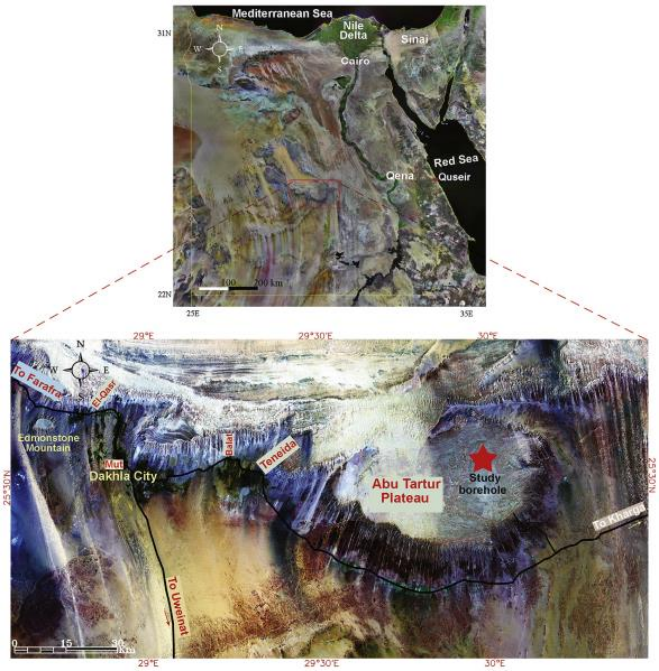

Figure 2. Satellite image of the Abu Tartour Plateau [23]

The Abu Tartour deposit is the largest and thickest phosphate deposit in Egypt, with a surface area of about 1200 km^2. The sectors that make up the plateau are as follows: Areas in the Maghrabi-Liffiya, Maghrabi, El Zayat, Wadi El Battikh, El Sebaiya, and Ain Amur [24].

In Figure 3, the age, lithology, and thickness of the general succession records of the Formation are depicted from top to bottom. The Duwi Formation, which is present in the study area, is composed of Lower Phosphorite, Middle Shale, and Upper Phosphorite elements [25].

The lower of the three phosphate sections that make up the Duwi Formation, with an average thickness of 3.5 meters and a percentage content of P_2O_5 varying from 17.9% to 29.9%, is the most economically significant. Its thickness can range from 0.70 to 10 meters.

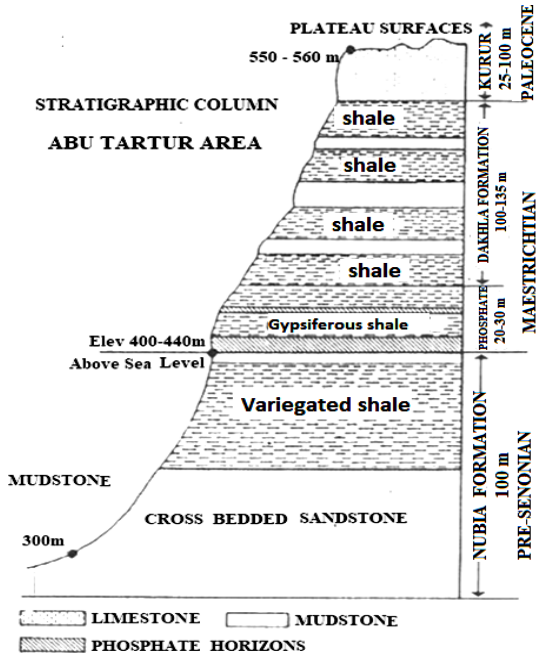

Figure 3. Stratigraphic column in the Abu Tartour area [23]

Black shale makes up the middle section, whereas the upper member is uneconomic. It has a thickness of 3-6 m, is interspersed with 2 thin phosphate beds, and has a P_2O_5 composition of less than 15%.

Under the microscope, two main components were found in the examined phosphorite samples from the study area: non-phosphatic components (calcite, dolomite, and other minerals used as cement) and phosphatic components (fragments of fish and shark bones, apatite, and iron oxides). The majority of phosphate grains are angular, elongated, and yellowish brown [24].

Phosphate ore occurs naturally at a lower grade and needs to be processed to a marketable P_2O_5 percentage for grade suitable for the phosphate industry. A high percentage of gangue minerals, such as silicates, carbonates, feldspar, calcite, mica and clays, are generally not accepted. In the majority of fertilizer industries, it is typical to find ores with P_2O_5 content equal to or greater than 30%, CaO/P_2O_5 ratios are less than 1.6, MgO concentrations are less than 1%, and Al_2O_3 and Fe_2O_3 concentrations are not exceeding 2.5%.

2. Modelling techniques used in this study

2.1. Decision Tree

The Decision Tree (DT) technique, as depicted in Figure 4, uses a flowchart representing a tree for categorizing data. A flexible method called decision trees is capable of learning from a large amount of training data [13], [26]. The DT is easier to understand than other data-driven approaches and does not require a deep understanding of calculations. However, it frequently results in substantial discrepancies between expectations and actual outcomes. The DT is more effective than estimating numerical variables for forecasting category features [13], [27]. Figure 5 shows how a decision tree is created.

The top node of a tree, or the root node, stands in for the sample being examined. A node splits when it is divided into smaller nodes; when a sub-node can be split into more nodes, it is referred to as a decision node. Tree nodes known as leaf nodes, do not have extra split nodes.

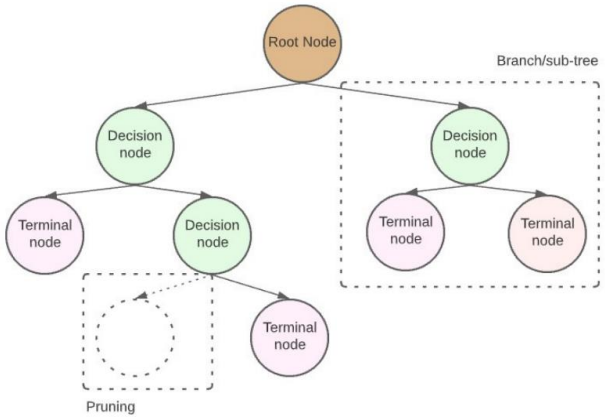

Figure 4. Decision Tree approach [13]

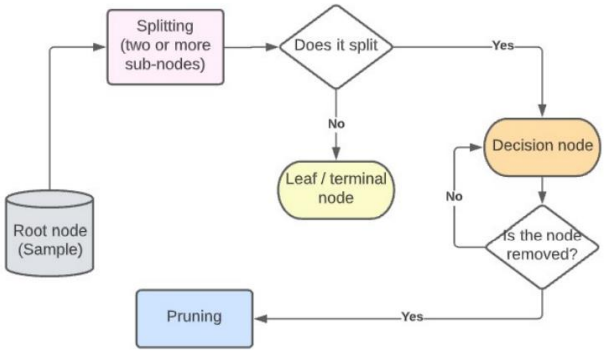

Figure 5. Decision Tree flowchart [13]

Pruning, which is the opposite of splitting and is done to avoid over-fitting, is the process of deleting sub-nodes from a decision node.

2.2. Support Vector Machine

To analyze data for classification, regression, and prediction, a non-parametric technique known as Support Vector Regression (SVR) can be used. It belongs to a class of supervised learning models that use connected learning algorithms. It is not surprisingly that artificial intelligence techniques have been monitored by researcher lately. Vepnayk introduced and demonstrated his ability to foresee problems with nonlinear systems in 1990 [14], [28]. The outcomes demonstrate the potential of this method in expanding and overcoming noise and the lack of data [14], [29], [30]. Similar to linear regression models, SVR models use a linear function to roughly represent the regression function. SVR seeks for a so-called insensitive loss function represented by an Equation, as opposed to linear regression, which aims to minimize the squared error, which may be greatly affected by a single observation out of phase with the overall trend (1):

$$L\varepsilon = \left(y,\left(x\right)\right) = \begin{cases} 0, & if \left|y - f\left(x\right)\right| < \in \\ \left|y - f\left(x\right)\right|, & if\ otherwise \end{cases}. \quad (1)$$

Reducing the influence of outliers on the regression model is one of the main justifications for adopting SVR. When evaluating the contribution of each data point to the total loss, an error threshold is used. Remaining data points that are below this cutoff point may not contribute to the overall loss.

SVR evaluates model parameters using a penalty term. The objective function can be described as a whole and represented by Equation (2):

$$J = C\sum_{i=1}^{n} L_{\in}\left(y, f\left(x\right)\right) + 0.5\left\|\beta\right\|^2 . \quad (2)$$

For a particular data point, it may show that the prediction function is:

$$f\left(x\right) = \beta_0 + \sum_i \alpha_i x_i^T x_i . \quad (3)$$

A kernel function (xi, x) that represents the dot product in higher dimensions and thus reflects non-linear relationships in the data, may be used in place of the dot product to replace the dot product. SVR models are flexible and most durable in the face of outliers and scant data, despite their complexity. SVR uses a variety of kernel functions to solve linear and non-linear regression problems. SVR has several advantages. However, it has some disadvantages, including the lack of a probabilistic prediction method and the need for the kernel function to be a positive-definite continuous symmetric function [14], [30].

2.3. Gaussian Process Regression

In the past, the Gaussian process has been used for forecasting in various domains of engineering and science [31]-[35]. A Gaussian process, according to Rasmussen and Williams, is a group of random variables that have the same joint Gaussian distribution when there are a finite number of them. The mean and covariance functions can be used to represent a Gaussian process as follows:

$$f \sim GP\left(m, k\right), \quad (4)$$

where:

m – the mean function;

k – the covariance function.

The mean and covariance will be a vector and a matrix, respectively, for a multivariate dataset. In most real problems, the mean value is assumed to be zero, i.e., $m(x) = 0$. If the training dataset consists of N number of samples with d dimension as $x_1, x_2,\ldots,x_d$ and the scalar target t, then the training data can be represented as $D = \{(x_i, t_i), i = 1,\ldots,N\}$. The target value can be determined as $t_i = f(\mathrm{x_i}) + \epsilon_i$, where ϵ_i – Gaussian noise with zero mean and variance, σ_n^2.

The value of the hypothetical Gaussian process f^* at the observation point can be used to estimate the target, t^*, if the observation of the test data is represented by x^*. This can be obtained as:

$$\begin{Bmatrix} t \\ f^* \end{Bmatrix} = GP\left(0, \begin{bmatrix} K\left(X, X\right) + \sigma_N^2 I_N & k\left(x^*\right) \\ k\left(x^*\right)^2 & k\left(x^*, x^*\right) \end{bmatrix}\right), \quad (5)$$

where:

t – the joint normality of the training target value and is given by $t = \left[t_i\right]_{i=1}^{N}$;

X – the joint normality of training observation and is given by $X = \left[x_i\right]_{i=1}^{N}$;

I_N – the identity matrix of size $N \times N$;

$k(x^*)$ – the vector of covariance between testing observation and all training observation and is given by:

$$k\left(X, X\right) = \Delta\begin{bmatrix} k\left(x_1, x_1\right) & k\left(x_1, x_2\right) & \cdots & k\left(x_1, x_N\right) \\ k\left(x_2, x_2\right) & k\left(x_2, x_2\right) & \cdots & k\left(x_1, x_N\right) \\ \vdots & \vdots & \ddots & \vdots \\ k\left(x_N, x_n\right) & k\left(x_n, x_2\right) & \cdots & k\left(x_N, x_N\right) \end{bmatrix}. \quad (6)$$

Thus, by conditioning the training samples, the predictive distribution model can be obtained. This is given by:

$$p\left(f^* \middle| x^*, D\right) = GP\left(f^* \middle| \mu^*, \sigma^{*2}\right), \quad (7)$$

where:

μ^* – the mean prediction.

The mean prediction can be estimated as:

$$\mu^* = k\left(x^*\right)^T \cdot \left(K\left(X, X\right) + \sigma_N^2 I_N\right)^{-1} \cdot t , \quad (8)$$

where:

σ^* – the variance prediction.

The variance prediction can be estimated as:

$$\sigma^{*2} = \sigma_N^2 - k\left(x^*\right)^T \cdot \left(K\left(X, X\right) + \sigma_N^2 I_N\right)^{-1} \cdot k\left(x^*\right) + k\left(x^*, x^*\right). \quad (9)$$

From the above equations, it is seen that the mean prediction is a linear combination of the observed target. The variance depends only on the observed inputs and not on the observed target. This is one of the Gaussian distribution properties.

2.4. Artificial Neural Network

A well-known Machine Learning approach called an Artificial Neural Network (ANN) aims to connect based on the replicate of human brain activity. An ANN can recreate a variety of human behavioral functions performed by a limited number of layers with various types of processing units called neurons [36], [37]. Input, hidden and output are three layers of ANN structure. The connection between the output and input layers is provided by hidden layers. ANN has typically been used for pattern identification, forecasting, estimation, optimization, and building links between complex features of variables. The advantage of ANN is that, even if the precise link between inputs and outputs is unknown, it is no need to have prior knowledge of object's qualities. Without any form of physical intervention, ANN can be used to understand relationships and extract the precise pattern between output and input variables without any further explanation. It can also find the exact performance between outputs and inputs from instances [37], [38]. This research uses ANN to predict the phosphate ore grade.

2.5. Ordinary kriging (OK)

Ordinary kriging is a popular multidimensional interpolation technique $\hat{y}\left(x_0\right)$ in which the value of a variable y at the exact location x is expected based on known sample values $\left\{\left(x_i, y_i\right)\right\}_{i=1}^{m}$ [39], [40], [41].

$$\hat{y}\left(x_0\right) = \sum_{i=1}^{m} \lambda_i y\left(x_i\right), \quad (10)$$

where:

$\hat{y}\left(x_0\right)$ – the kriging prediction at the unknown location;

x_0, $y(x_i)$ – the known value at location x_i;

λ_i – the weighting factor for $y(x_i)$.

The kriging prediction error is:

$$\hat{y}\left(x_0\right) - y\left(x_0\right) = R\left(x_0\right) = \sum_{i=1}^{m} \lambda_i y\left(x_i\right) - y\left(x_0\right), \quad (11)$$

where:

$R(x_0)$m – the prediction error;

$y(x_0)$ – the unknown true value at x_0.

The prediction error mean can be equal to zero for an unbiased estimate, so:

$$E\{R(x_0)\} = 0\,, \tag{12}$$

and

$$\sum_{i=1}^{m} \lambda_i = 1\,. \tag{13}$$

The reader is invited to read more information on the ordinary kriging method and its use [35], [38].

2.6. GIS modeling

In the presented research, the spatial distribution of phosphate ore elements is studied using a Triangulated Irregular Network (TIN). TIN represents a surface as a network of adjacent, non-overlapping triangles of different sizes and proportions, formed by a set of irregularly spaced points connected by lines. Each triangle node contains the *x*, *y*, and *z* values [42]. The surface analysis using TINs has several advantages, including the maintenance of original sample points, which are a useful way to assess the accuracy of a model. Secondly, TIN is a useful tool for storing surface characteristics such as terrains with significant topographical variations due to variable density of triangles. Determining the elevation, aspect, slope, and line of sight between places is also simplified due to the data format. The TIN data structure is widely used in applications including volumetric computation for roadway construction, drainage studies for land development, and visualization of urban patterns as a result of a combination of these elements [43].

3. Data description and preparation

The datasets in this study have been collected from 226 drill holes. These datasets include coordinates, elevations, ore thickness and chemical analysis of samples taken from boreholes (P_2O_5 %, I.R. %, Fe_2O_3%, and Fe total %). Table 1 presents a summary of the statistical evaluation of all data used in this paper. Thickness ranges from1.2 to 11.35 meters, I.R.% ranges from 2.37 to 29.46, Fe total % ranges from 2.16 to 4.73, Fe_2O_3 % ranges from 1.09 to 4.36 and P_2O_5 % ranges from 14.16 to 30.16, kurtosis and skewness with thickness of I.R. %, Fe total %, Fe_2O_3 %, and P_2O_5 % are more than -1 and less than 3. Therefore, this means that these variables are normally distributed and there is no need to extract any values from them.

It is extremely important to study the effect of each parameter on the desired result before constructing the model. Figure 6 shows that the phosphate ore grade is related to the input parameters (coordinates, thickness, I.R., Fe total%, and Fe_2O_3 %). The parameters which have a great effect on the estimation of phosphate ore grade in this study are I.R., Fe total %, and Fe_2O_3 %.

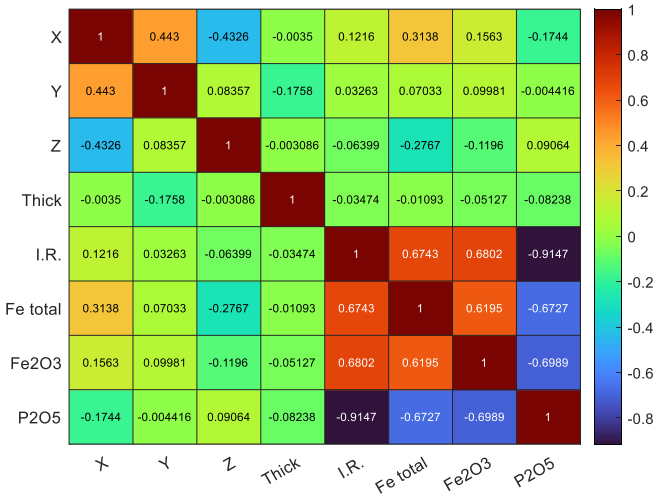

Figure 6. Heatmap of the input and output parameters

The obtained datasets are split into two sets before development and assessment of Machine Learning approaches to predict the phosphate reserve. The first batch of 181 datasets out of 226 (80%) is used to train the models, and 45 datasets (20%) are used to assess the models' performance. Additionally, to create ANN models, all data are normalized between -1 and 1. Tables 2 and 3 show the training and validation data ranges.

4. Results and discussion

This paper evaluates four techniques of Machine Learning Algorithms, namely an Optimizable Decision Tree, an Optimizable Support Vector Machine, an Optimizable Gaussian Process Regression, and an Artificial Neural Network in addition to geostatistical and GIS modeling for estimating phosphate ore grade of one of the most important areas in the Egyptian Western Desert.

Table 1. Statistical evaluation of all datasets used in this study

	X, m	*Y*, m	*Z*, m	Thick, m	I.R. %	Fe total %	Fe_2O_3 %	P_2O_5 %
Kurtosis	-0.80695	-0.42959	28.99508	1.418381	1.481829	0.427337	2.857056	0.046297
Skewness	0.037443	0.115056	-2.30276	1.080157	1.383106	0.638287	1.226066	-0.79391
Minimum	513847.7	299496.5	456.1	1.2	2.37	2.16	1.09	14.16
Maximum	523112.1	307886.9	599.7	11.35	29.46	4.73	4.36	30.16

Table 2. Statistical evaluation of training and validation data

				Training data				
	X, m	*Y*, m	*Z*, m	Thick, m	I.R. %	Fe total %	Fe_2O_3 %	P_2O_5 %
Kurtosis	-0.77	-0.47	33.31	-0.99	1.59	0.41	2.46	0.15
Skewness	0.14	0.01	-2.64	-0.17	1.5	0.65	1.19	-0.94
Minimum	514945.1	299496.5	456.1	1.2	3.31	2.16	1.09	14.16
Maximum	523072.6	307886.9	599.7	5.55	29.46	4.73	4.36	29.53
				Validation data				
Kurtosis	-1.37	-0.02	1.96	-0.34	0.35	-0.28	-0.59	-0.29
Skewness	0.1	0.2	-0.48	0.89	0.59	0.43	0.35	0.04
Range	9115.9	6992.9	50.5	5.65	22.55	1.56	1.27	14.59
Minimum	513847.7	300285.9	516.2	5.7	2.37	2.28	1.31	15.57
Maximum	522963.6	307278.8	566.7	11.35	24.92	3.84	2.58	30.16

Table 3. Coefficients of Equation (14)

i	$w_{i,1}$	$w_{i,2}$	$w_{i,3}$	$w_{i,4}$	$w_{i,5}$	$w_{i,6}$	$w_{i,7}$	b	w_h
1	0.88511	-0.97043	0.25898	-1.3975	-0.79156	-0.39851	0.28689	-2.2853	0.8456
2	0.12365	0.3935	-1.583	-0.00199	0.83621	0.17812	0.64085	-1.6578	-0.41268
3	-0.35614	1.2977	-0.9042	0.52964	-1.0373	0.43595	0.58263	0.70813	0.77139
4	0.79143	0.070081	-0.61212	0.86063	1.0003	-0.64327	-0.84774	-0.79095	0.12923
5	1.0237	0.71121	0.19278	-1.0069	0.50419	-0.48046	0.74291	0.22022	-0.89397
6	-0.90217	-1.7268	0.0038	1.2864	-1.0728	1.0959	-0.09019	0.15027	-0.59498
7	1.1847	0.41613	0.46559	0.22019	-0.03826	-0.89866	1.0941	0.50657	-0.0354
8	0.25475	-0.98609	1.259	-0.59728	-0.51823	0.28332	-0.58068	-0.78443	0.57668
9	-0.49888	-0.47752	-0.44777	0.073188	1.1065	-1.0884	1.1271	-0.9801	0.46722
10	-1.6555	1.0745	-0.20943	0.63788	0.21491	0.37722	0.7375	-1.2776	-0.78096
11	-0.26025	0.86918	-0.78529	1.1097	-0.12376	0.91988	-0.72297	-1.6094	0.19306
12	0.49886	0.49733	0.14498	-0.5429	-1.8723	0.093522	0.078622	2.0134	0.29664

For all four Machine Learning techniques, the datasets are split into 80% for model training and 20% for model performance testing.

The grade phosphate ore is estimated using an ANN model in this study as a function of coordinates, thickness, I.R. %, Fe total %, Fe_2O_3 %, and P_2O_5 %. Three layers form the model basis, as seen in Figure 7. Seven neurons serve as inputs in the input layer, the first layer. The hidden layer, which is the second layer, consists of 12 neurons. The 3rd layer is the output layer, which has one neuron for estimating the output parameter, the phosphate ore grade. The Levenberg-Marquardt technique is used as a training algorithm, a tan sigmoid function as a transfer function for the middle-hidden layer. To achieve this goal, a pure linear function is studied as an output function.

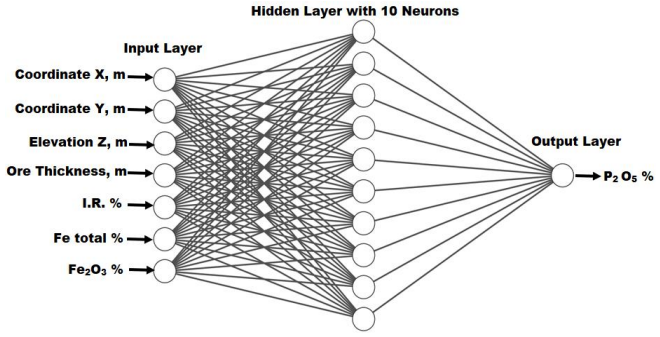

Figure 7. Architecture of the proposed ANN model for calculating the phosphate ore grade

The phosphate ore grade can be calculated using the following ANN-based mathematical model with the coefficients presented in Tables 3 and 4.

$$P_2O_5 = 22.16 + 8\left[\sum\left(\frac{2w_{hi}}{1+e^{-2S_{i,j}}} - 1\right) + 0.005052\right]; \quad (14)$$

$$S_{i,j} = b_i + \sum w_{i,j}\left(m_j x_j - a_j\right), \quad (15)$$

where:

$w(i, 1)$, $w(i, 2)$, $w(i, 3)$, $w(i, 4)$, $w(i, 5)$, $w(i, 6)$, $w(i, 7)$ – represent the weights of neuron i and inputs 1, 2, 3, 4, 5, 6, and 7, respectively;

b_i – the bias of neuron i.

The weight of hidden neuron i is represented by w_{hi}.

The results show that four techniques can be applied to estimate phosphate content with reasonable accuracy. The estimation results of four Machine Learning techniques for validation and training data, respectively, are shown in Tables 5 and 6. They include the RMSE, correlation coefficients and MAE. For training data, the RMSE for ANN, Optimizable DT, Optimizable SVM, and Optimizable GPR are 1.26, 1.49, 1.42, and 1.35, respectively, and the correlation coefficients between expected values and real values are 0.933, 0.921, 0.927, and 0.933. For validation data, the correlation coefficients between actual and predicted values are 0.893, 0.872, 0.922, and 0.927 with RMSE of 1.30, 1.59, 1.24, and 1.20 for ANN, Optimizable DT, Optimizable SVM, and Optimizable GPR, respectively.

Table 4. Coefficients of Equation (15)

m_i	0.000216	0.000238	0.013928	0.197044	0.073828	0.77821	0.611621
a_i	111.9295	72.39028	7.352368	1.236453	1.174972	2.680934	1.666667

Table 5. Evaluation of Machine Learning techniques used in this study for training data

Technique	RMSE	MAE	R
ANN	1.268	3.9	0.933
Optimizable Tree	1.4932	1.1671	0.921
Optimizable SVM	1.4202	1.0695	0.927
Optimizable GPR	1.35	0.98373	0.933

Table 6. Evaluation of Machine Learning techniques used in this study for validation data

Technique	RMSE	MAE	R
ANN	1.3	4.2	0.893
Optimizable Tree	1.5925	1.2689	0.872
Optimizable SVM	1.2491	0.95939	0.922
Optimizable GPR	1.2094	0.93395	0.927

The most efficient technique for estimating phosphate content is the Optimizable GPR, which gives correlation coefficients (R) of 0.933 and 0.927 with MAE of 0.983 and 0.933 for the training data and validation data, respectively. For a quick estimation of phosphate ore grade, the ANN-based mathematical model can be used. The proposed models can be applied to any other data within the range used in this study.

Figures 8-11 show the predicted phosphate ore grade versus actual phosphate ore grade for different Machine Learning models (Optimizable DT, Optimizable SVM, Optimizable GPR, and ANN) studied in this paper.

These plots are important for showing the accuracy of each technique. Since the calculated values of phosphate ore grade are close to the actual values, the model is more accurate.

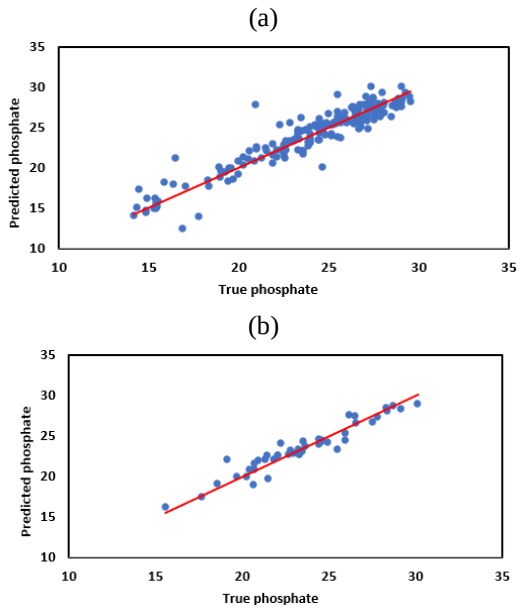

Figure 8. Cross plots of ANN model for training (a) and validation (b) data

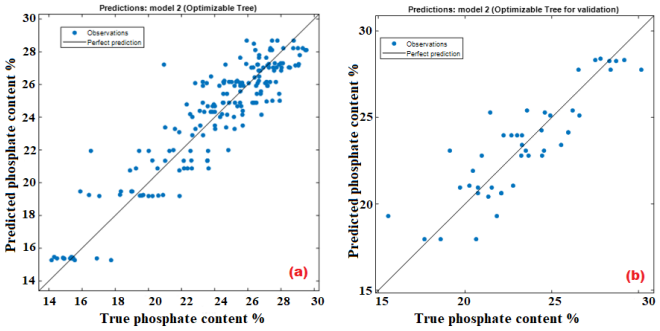

Figure 9. Cross plots of ODT model for training (a) and validation (b) data

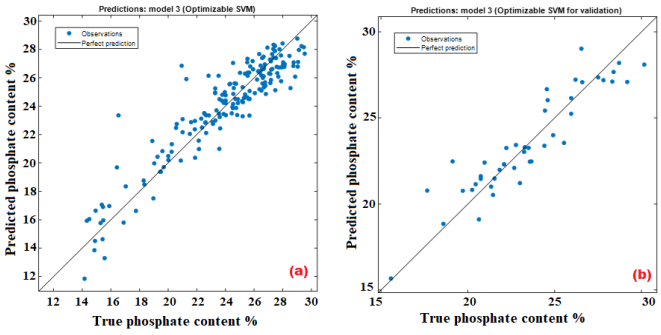

Figure 10. Cross plots of OSVM model for training (a) and validation (b) data

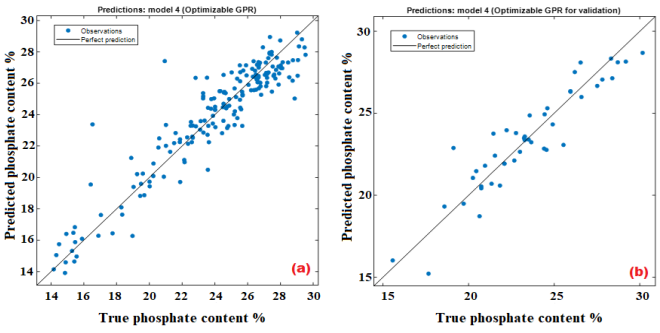

Figure 11. Cross plots of OGPR model for training (a) and validation (b) data

In other words, since the angle between the straight lines drawn on these plots and *x*-axes is close to 45°, the developed model is more accurate. In this paper, four advanced Machine Learning techniques are used to predict the phosphate ore grade. These plots show reasonable correlation coefficients between real and estimated values with correlation coefficients ranging from 0.921 to 0.933 for training data and from 0.872 to 0.927 for validation data.

5. GIS analysis of the Abu Tartour phosphate ore elements

The interpolated Triangulated Irregular Network (TIN) is used to construct an iso-chemical map for the phosphate ore elements distributed at the Abu Tartour phosphate ore mine as shown in Figure 12. This TIN has been classified where each class has a specific color and represents a specific percentage of the phosphate ore element. The percentage of P_2O_5 at the Abu Tartour phosphate ore mine ranges from 14.16% to 30.16%, while the average percentage of P_2O_5 for the entire mine is 23.86%.

The areas with the highest percentage of P_2O_5 are distributed in the southwestern part of the mine, in these areas phosphate can be used directly without ore beneficiation when the grade is above 27%. And most of the area has a high percentage of P_2O_5 ranging from 23 to 30%, except for a small part in the eastern area with a grade of less than 23%. The percentage of insoluble residual elements at the Abu Tartour mine ranges from 2.37 to 29.46%, while the average percentage of insoluble residual elements for the whole mine is 10.25%.

The high percentage of I.R. is concentrated in the northeastern part of the area, while a low percentage is in the middle part of the area. The percentage of Fe_2O_3 at the Abu Tartour phosphate ore mine ranges from 1.09 to 4.36%, while the overall average percentage of Fe_2O_3 at the mine is 2.02%. The percentage of Fe at the Abu Tartour phosphate ore mine ranges from 2.16 to 4.73%, while the average percentage of Fe for the whole mine is 3.03%. The high percentage of Fe is distributed in the area from the center to the east, while the areas with the lowest percentage of Fe are concentrated in the western part of the Abu Tartour area. The percentage of Fe at the Abu Tartour mine is high except for some areas extended in the western part of the mine. The phosphate thicknesses at the Abu Tartour phosphate ore mine ranges from 1.2 to 11.35, while the average phosphate thicknesses for the whole mine is 4.34. The low ore thickness is concentrated in the middle part of the mine, while the area of the highest ore thickness is in the northwestern part.

6. Geostatistical analysis

6.1. Construction of Variograms

In Figure 13, global variogram models are constructed for each parameter in the studied area, each variogram model has its own special parameters describing the variability of P_2O_5 %; I.R. %; thickness; Fe_2O_3 %; and Fe % within the studied area. These variogram parameters are very important and were used when creating kriging models (in section 6.2) for mapping analysis (Fig. 14) that reveals the spatial distribution for P_2O_5 %; I.R. %; thickness; Fe_2O_3 %; and Fe % and these parameters are summarized in Table 7.

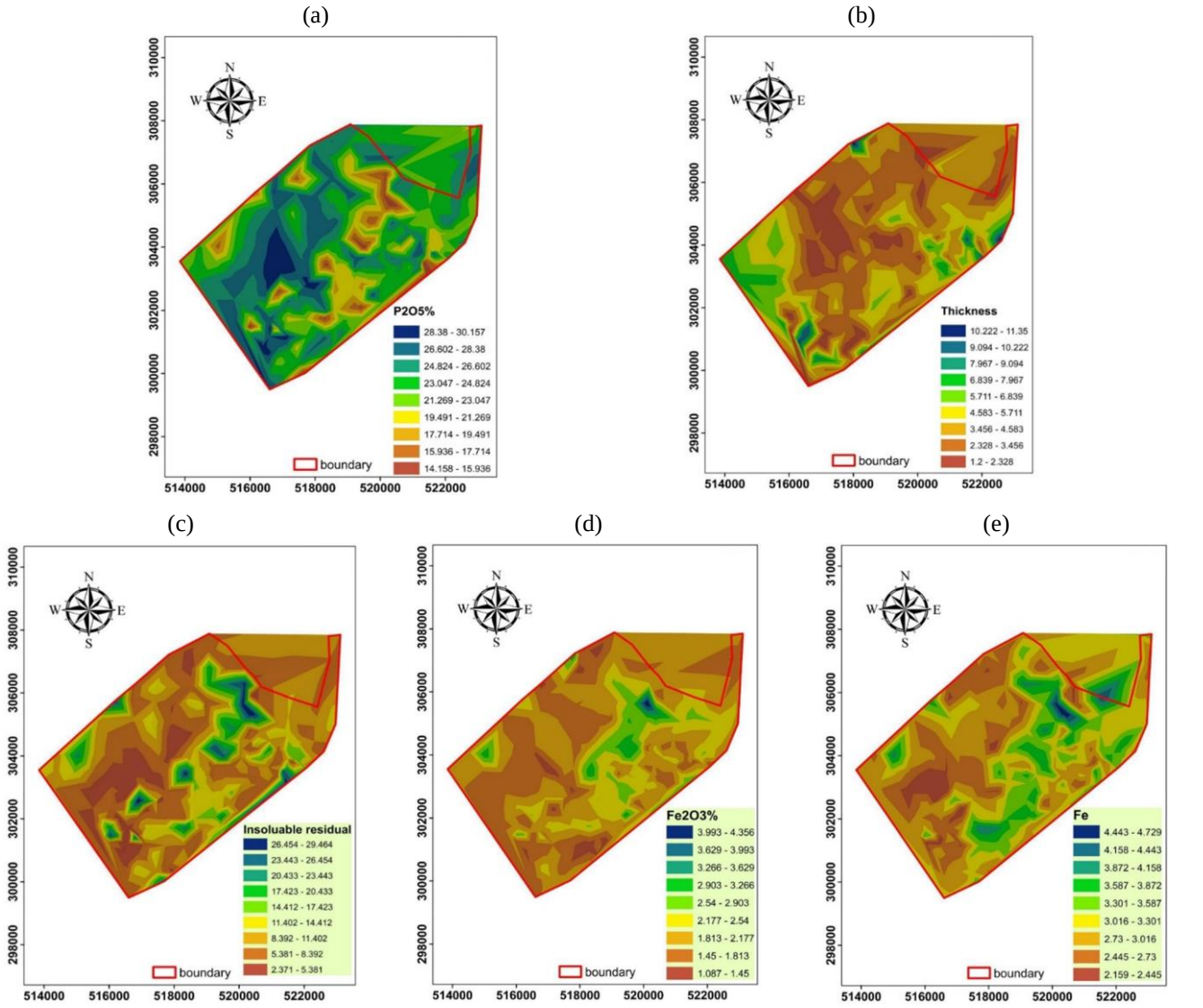

Figure 12. Spatial distribution of phosphate ore elements at the Abu Tartour mine: (a) P_2O_5 % distribution; (b) thicknesses distribution; (c) distribution of insoluble residual elements; (d) Fe_2O_3 % distribution; (e) Fe % distribution

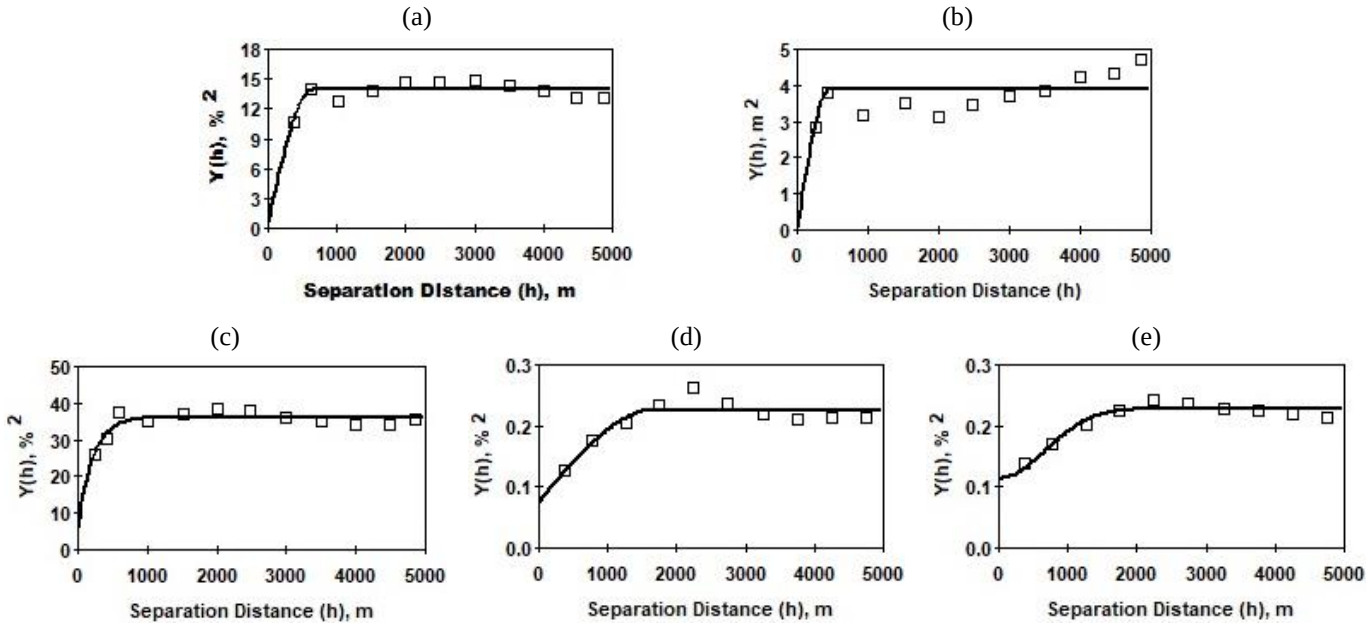

Figure 13. Variogram models for phosphate ore elements in the Abu Tartour Area: (a) Spherical Model for P_2O_5 %; (b) Spherical Model for thickness; (c) Exponential Model for I.R. %; (d) Spherical Model for Fe_2O_3 %; (e) Gaussian Model for Fe %

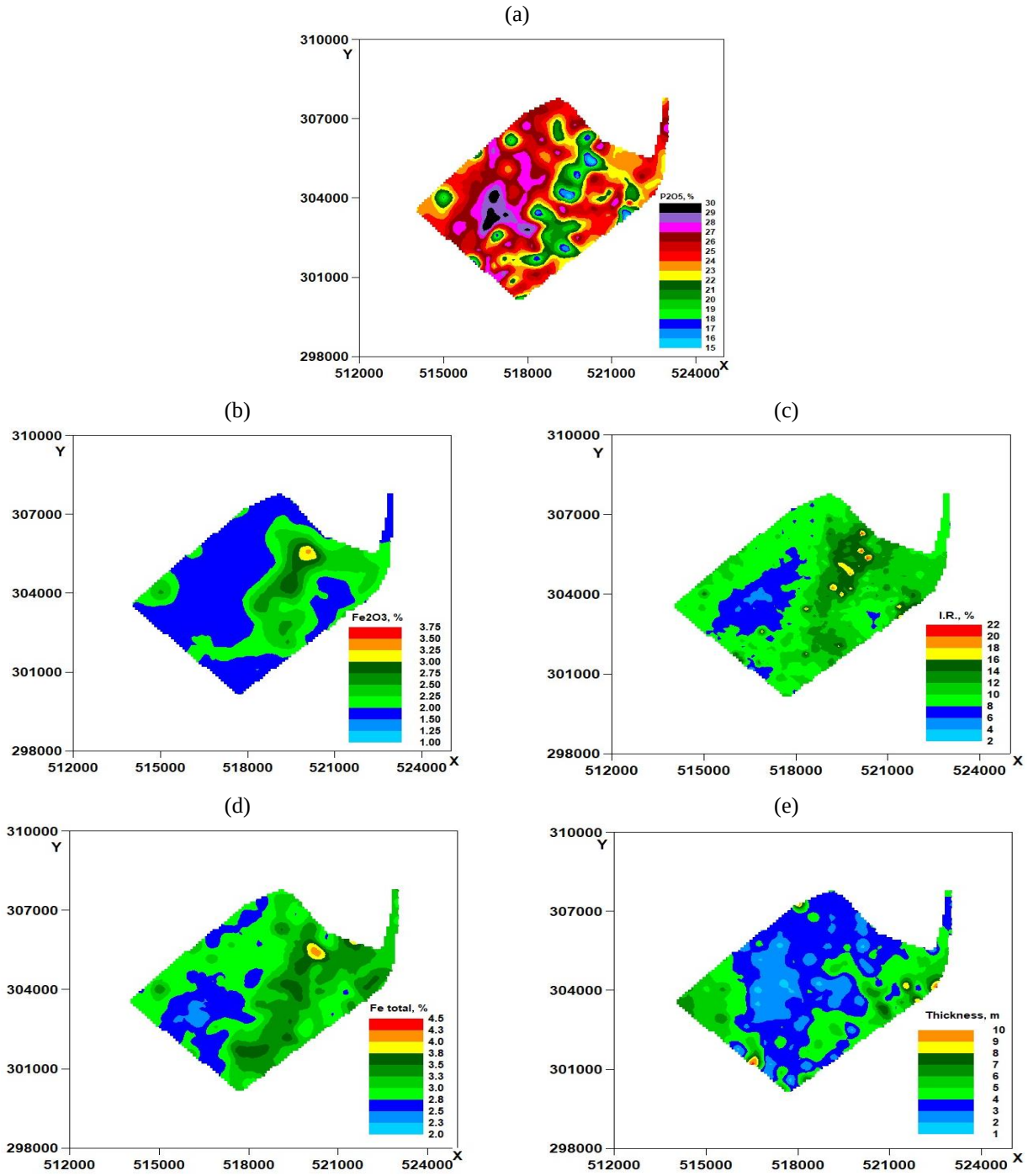

Figure 14. Kriging Models of the Abu Tartour phosphate ore elements: P_2O_5 %, I.R. % distribution, Thickness, Fe_2O_3 % and Fe distribution

Table 7. Variogram Parameters of the datasets used in the study area

Variogram parameters	P_2O_5	Thickness	I.R.	Fe_2O_3	Fe %
Type	Spherical	Spherical	Exponential	Spherical	Gaussian
Direction	Global	Global	Global	Global	Global
Range, m	640	460	630	1690	1628
Nugget effect(C_0), $\%^2$	0.67%^{2}	0.05 m^2	5.6%^{2}	0.08%^{2}	0.1%^{2}
Sill (C), $\%^2$	13.9%^{2}	3.9 m^2	36.2%^{2}	0.23%^{2}	0.23%^{2}
Screen Effect Ratio C_0/C	0.05	0.01	0.15	0.35	0.43

6.2. Kriging models

According to the variogram model selected for each parameter, ordinary kriging is used to interpolate locations where no samples were taken by creating a map analysis that reveals the spatial distribution of P_2O_5 %, I.R. %, Thickness, Fe_2O_3, and Fe % in the studied area as shown in Figure 14. Maps are classified into different colures; each colure represents a definite range of percentage of P_2O_5 %; I.R. %; Thickness; Fe_2O_3; and Fe % as shown in Figure 14.

Most of the area has a high percentage of P_2O_5, except for a small part in the central area, where the P_2O_5 distribution has a high percentage variance, but is still within the ac-

ceptable range for the used ore. The high percentage of I.R. is concentrated in the north-eastern part of the area, while the low percentage is in the middle part of the area. Low ore thickness, concentrated in the middle part of the area, exceeds the limits in the eastern and western directions. The central part to the east of the area has a high percentage of Fe_2O_3, while the rest of the area has an acceptable percentage of Fe_2O_3. Finally, a high percentage of Fe is in the whole area, except for small parts in the southern and northern directions. Also, maps indicate that most of the P_2O_5 %, thickness, and Fe % are suitable for phosphate production processes, except for small pockets that require little attention at the mining stage. In general, phosphate ore and its impurities in the studied area are suitable for P_2O_5 production for various purposes.

7. Conclusions

In this work, the phosphate ore grade (P_2O_5 %, Fe total %, I.R. %, and Fe_2O_3 %) in the Abu Tartour mine area, Western Desert, Egypt, has been predicted using the GIS analysis, Triangulation Irregular Network (TIN) method, Geostatistical-based modeling, and four techniques of Machine Learning Algorithms (MLA), namely, Optimizable Decision Tree (ODT), Optimizable Support Vector Machine (OSVM), Optimizable Gaussian Process Regression (OGPR) and Artificial Neural Network (ANN). The following conclusions can be drawn:

– four Machine Learning models (Optimizable DT, Optimizable SVM, Optimizable GPR, and ANN) may be used to estimate the phosphate ore grade with reasonable accuracy;

– the most efficient technique for estimating phosphate content is Optimizable GPR, which gives correlation coefficients (*R*) of 0.933 and 0.927 with Mean Absolute Errors (MAE) of 0.983 and 0.933 for training data and validation data, respectively;

– the proposed ANN-based model (white box) can be used for quick estimation of phosphate ore grade with reasonable accuracy;

– the proposed white box model can be applied for any other data within the range used in this study;

– constructed variogram models, kriging, and TIN have provided a clear understanding of all the elements distributed in the Abu Tartour phosphate ore, which can be very useful at the planning and mining stages;

– GIS analysis and geostatistical technique have proved that the P_2O_5 %, thickness, and Fe % are suitable for the phosphate production processes, except for small pockets that require little attention at the mining stage.

Acknowledgements

The authors gratefully acknowledge research funding from Al-Azhar University. This work was fully supported by the research funding of Al-Azhar University.

References

[1] Schalkoff, R.J. (1997). *Artificial neural networks*. New York, United States: McGraw-Hill, Computer Science Series, 422 p.

[2] Kapageridis, I.K. (1999). *Application of artificial neural network systems to grade estimation from exploration data*. PhD Thesis. Nottingham, United Kingdom: University of Nottingham.

[3] Zhang, G., Patuwo, B.E., & Hu, M.Y. (1998). Forecasting with artificial neural networks: The state of the art. *International Journal of Forecasting*, *14*(1), 35-62. https://doi.org/10.1016/S0169-2070(97)00044-7

[4] Dave, V.S., & Dutta, K. (2014). Neural network-based models for software effort estimation: A review. *Artificial Intelligence Review*, *42*(2), 295-307. https://doi.org/10.1007/s10462-012-9339-x

[5] Abiodun, O.I., Jantan, A., Omolara, A.E., Dada, K.V., Mohamed, N.A.E., & Arshad, H. (2018). Review article state-of-the-art in artificial neural network applications: A survey. *Heliyon*, (4), e00938. https://doi.org/10.1016/j.heliyon.2018.e00938

[6] Zador, A.M. (2019). A critique of pure learning and what artificial neural networks can learn from animal brains. *Nature Communications*, (10), 3770. https://doi.org/10.1038/s41467-019-11786-6

[7] Samanta, B., Bandopadhyay, S., & Ganguli, R (2006). Comparative evaluation of neural network learning algorithms for ore grade estimation. *Mathematical Geology*, *38*(2), 175-197. https://doi.org/10.1007/s11004-005-9010-z

[8] Bakarr, J.A., Sasaki, K., Yaguba, J., & Karim, B.A. (2016). Integrating artificial neural networks and geostatistics for optimum 3D geological block modeling in mineral reserve estimation: A case study. *International Journal of Mining Science and Technology*, *26*(4), 581-588. https://doi.org/10.1016/j.ijmst.2016.05.008

[9] He, S., & Li, F. (2021). Artificial neural network model in spatial analysis of geographic information system. *Artificial Intelligence and Edge Computing in Mobile Information Systems*, 1166877. https://doi.org/10.1155/2021/1166877

[10] Sarkar, B.C., Singh, R.K., Ray, D., Kumar, A., Sinha, P.K., & Sarkar, V. (2017). Iron ore grade modelling using geostatistics and artificial neural networks. *Iron Ore Conference*, (3).

[11] Mousa, B.G., Embaby, A.E., & Osman, M.E. (2016). *Applications of GIS in operations of open cast mining*. Berlin, Germany: LAP Lambert Academic Publishing, 132 p.

[12] Kaplan, U.E., & Topal, E. (2020). A new ore grade estimation using combine machine learning algorithms. *Minerals*, (10), 847. https://doi.org/10.3390/min10100847

[13] El Maghraoui, A., Ledmaoui, Y., Laayati, O., El Hadraoui, H., Chebak, A. (2022). Smart energy management: A comparative study of energy consumption forecasting algorithms for an experimental open-pit mine. *Energies*, (15), 4569. https://doi.org/10.3390/en15134569

[14] Zaki, M.M., Chen, S., Zhang, J., Feng, F., Khoreshok, A.A., Mahdy, M.A., & Salim, K.M.A. (2022) Novel approach for resource estimation of highly skewed gold using machine learning algorithms. *Minerals*, (12), 900. https://doi.org/10.3390/min12070900

[15] Patel, A.K., Chatterjee, S., & Gorai, A.K. (2019). Development of a machine vision system using the support vector machine regression (SVR) algorithm for the online prediction of iron ore grades. *Earth Science Informatics*, (12), 197-210. https://doi.org/10.1007/s12145-018-0370-6

[16] Dumakor-Dupey, N.K., & Arya, S. (2021). Machine learning – A review of applications in mineral resource estimation. *Energies*, (14), 4079. https://doi.org/10.3390/en14144079

[17] Gorai, A.K., Raval, S., Patel, A.K., Chatterjee, S., & Gautam, T. (2021). Design and development of a machine vision system using artificial neural network-based algorithm for automated coal characterization. *International Journal of Coal Science & Technology*, (8), 737-755. https://doi.org/10.1007/s40789-020-00370-9

[18] Samanta, B., Bandopadhyay, S., Ganguli, R., & Dutta, S. (2004). Sparse data division using data segmentation and Kohonen network for neural network and geostatistical ore grade modeling in Nome offshore placer deposit. *Natural Resources Research*, *13*(3), 189-200. https://doi.org/10.1023/b:narr.0000046920.95725.1b

[19] Abuntori, C.A., Al-Hassan, S., & Mireku-Gyimah, D. (2021). Assessment of ore grade estimation methods for structurally controlled vein deposits – A review. *Ghana Mining Journal*, *21*(1), 31-44. https://doi.org/10.4314/gm.v21i1.4

[20] Tahmasebi, P., & Hezarkhani, A. (2010). Comparison of optimized neural network with fuzzy logic for ore grade estimation. *Australian Journal of Basic and Applied Sciences*, *4*(5), 764-772.

[21] Domingos, P. (2012). A few useful things to know about machine learning. *Communication of the ACM*, *55*(10), 78-87. https://doi.org/10.1145/2347736.2347755

[22] Hellal, F., El-Sayed, S., Zewainy, R., & Amer, A. (2019). Importance of phosphate pock application for sustaining agricultural production in Egypt. *Bulletin of the National Research Centre*, *43*(1), 11. https://doi.org/10.1186/s42269-019-0050-9

[23] Ahmed, S., & Rizk, M.E. (2022). Highlights on the beneficiation trials of the Egyptian phosphate ores. *Journal of Engineering Sciences*, *50*(1), 1-21. https://doi.org/10.21608/jesaun.2021.100795.1083

[24] Schewe, M., Müller, P., Korte, T., & Herrmann, A. (1992). The role of phospholipid asymmetry in calcium-phosphate-induced fusion of human erythrocytes. *Journal of Biological Chemistry*, *267*(9), 5910-5915. https://doi.org/10.1016/s0021-9258(18)42640-3

[25] El-Shafeiy, M., Birgel, D., El-Kammar, A., El-Barkooky, A., Wagreich, M., Mohamed, O., & Peckmann, J. (2014). Palaeoecological and post-depositional changes recorded in Campanian-Maastrichtian black shales, Abu Tartur plateau, Egypt. *Cretaceous Research*, (50), 38-51. https://doi.org/10.1016/j.cretres.2014.03.022
[26] Elmaadawy, Kh.G., Ezz El Din, M., Khalid, A.M., & Seifelnasr, A.A. (2015). Mineral industry in Egypt – Part II Non-metallic commodities – phosphate rocks. *Journal of Mining World Express*, *4*(0), 1. https://doi.org/10.14355/mwe.2015.04.001
[27] Yu, Z., Haghighat, F., Fung, B.C.M., & Yoshino, H. (2010). A decision tree method for building energy demand modeling. *Energy Build*, (42), 1637-1646. https://doi.org/10.1016/j.enbuild.2010.04.006
[28] Cristianini, N., & Shawe-Taylor, J. (2000). An *introduction to support vector machines and other kernel-based learning methods*. Cambridge, United Kingdom: Cambridge University Press, 189 p. https://doi.org/10.1017/CBO9780511801389
[29] Steinwart, I., & Christmann, A. (2008). *Support vector machines*. Berlin/Heidelberg, Germany: Springer Science & Business Media, 610 p.
[30] Tipping, M. (2001). Sparse Bayesian learning and the relevance vector machine. *Journal of Machine Learning Research*, (1), 211-244.
[31] Archambeau, C., Cornford, D., Opper, M., & Shawe Taylor, J. (2007). Gaussian process approximations of stochastic differential equations. *Journal of Machine Learning Research*, (1), 1-16.
[32] Atia, M.M., Noureldin, A., & Korenberg, M. (2012). Enhanced Kalman filter for RISS/GPS integrated navigation using Gaussian process regression. *Proceedings of the Institute of Navigation International Technical Meeting*, 1148-1156.
[33] Chen, H.M., Cheng, X.H., Wang, H., & Han, X. (2014). Dealing with observation outages within navigation data using Gaussian process regression. *Journal of Navigation*, *67*(4), 603-615. https://doi.org/10.1017/S0373463314000010
[34] Bailer-Jones, C.A.L., Sabin, T.J., MacKay, D.J.C., & Withers, P.J. (1997). Prediction of deformed and annealed microstructures using Bayesian neural networks and Gaussian processes. *Proceedings of the Australasia Pacific Forum on Intelligent Processing and Manufacturing of Materials*, 913-919.
[35] Rasmussen, C.E., & Williams, C. (2006). *Gaussian processes for machine learning*. Cambridge, United States: MIT Press, 248 p. https://doi.org/10.7551/mitpress/3206.001.0001
[36] Nathan, D., Thanigaiyarasu, G., Vani, K., & India, C. (2016). Compasison of artificial neural network approach and data mining technique for the prediction of surface roughness in end milled components with texture images. *International Journal of Advanced Engineering Technology*, (592), 587.
[37] Duong, V.-H., Ly, H.-B., Trinh, D. H., Nguyen, T. S., & Pham, B. T. (2021). Development of Artificial Neural Network for prediction of radon dispersion released from Sinquyen Mine, Vietnam. *Environmental Pollution*, (282), 116973. https://doi.org/10.1016/j.envpol.2021.116973
[38] Mustafa, M.R., Rezaur, R.B., Saiedi, S., & Isa, M.H. (2012). River suspended sediment prediction using various multilayer perceptron neural network training algorithms – A case study in Malaysia. *Water Resources Management*, *26*(7), 1879-1897. https://doi.org/10.1007/s11269-012-9992-5
[39] Webster, R., & Oliver, M.A. (2007). *Geostatistics for environmental scientists*. Hoboken, United States: John Wiley & Sons Ltd, 318 p. https://doi.org/10.1002/9780470517277
[40] Isaaks, E., & Srivastava, R. (1989). *Applied geostatistics*. New York, United States: Oxford University Press, 582 p.
[41] Kennedy, K.H. (2009). *Introduction to 3D data*. Hoboken, United States: John Wiley & Sons Ltd, 332 p.
[42] Longley, P.A., Goodchild, M.F., Maguire, D.J., & Rhind, D.W. (2005). *Geographical information systems and science*. Chichester, United Kingdom: John Wiley & Sons Ltd.
[43] Kaplan, U.E., Dagasan, Y., & Topal, E. (2021). Mineral grade estimation using gradient boosting regression trees. *International Journal of Mining, Reclamation and Environment*, *35*(10), 728-742. https://doi.org/10.1080/17480930.2021.1949863

Підхід, заснований на алгоритмах машинного навчання, геостатистичному методі та ГІС-аналізі для оцінки вмісту фосфатної руди на руднику Абу Тартур, Західна пустеля Єгипту

А. Ембабі, А. Ісмаель, Ф.А. Алі, Х.А. Фараг, Б.Г. Муса, С. Гомаа, М. Ельвагі

Мета. Оцінка вмісту фосфатних руд у районі Абу Тартур, Західної пустелі Єгипту на основі використання чотирьох алгоритмів машинного навчання (MLA), геостатистичних методів (моделі варіограми і кригінгу) та ГІС-аналізу для отримання швидких та надійних результатів.

Методика. У цій статті застосовуються чотири методи машинного навчання, включаючи оптимізоване дерево рішень (ODT), оптимізовану машину опорних векторів (OSVM), оптимізовану регресію Гаусівського процесу (OGPR), штучну нейронну мережу (ANN). Побудовані моделі варіограми та крігінгу, а також ГІС-аналіз забезпечують чітке розуміння про всі елементи, які поширені у фосфатній руді Абу Тартур, і є дуже корисними на етапах планування та видобування.

Результати. Вміст фосфатів було оцінено з високою точністю за результатами чотирьох методів машинного навчання. Визначено, що найбільш ефективним методом оцінки вмісту фосфатів є оптимізований (OGPR) метод, який дає коефіцієнти кореляції (R) 0.933 і 0.927 при середніх абсолютних похибках (MAE) 0.983 і 0.933 для даних навчання та перевірки відповідно. Геостатистичні та ГІС-методи показали, що відсоток P_2O_5, потужність та відсоток Fe придатні для процесів видобування фосфатів, за винятком невеликих осередків, які потребують незначної уваги на етапі видобутку.

Наукова новизна. Вперше розроблено алгоритм швидкої оцінки вмісту фосфатної руди та забезпечено чітке розуміння розподілу різних складових у рудному тілі за допомогою різних методів.

Практична значимість. Оцінка вмісту, зазвичай, зводиться до апроксимації функції. Методи штучного інтелекту, зокрема вибраний тип AI-методів, можуть надати дійсну методологію для оцінки вмісту, а запропоновані моделі можна застосовувати до будь-яких інших даних у діапазоні, який використовується в цьому дослідженні.

Ключові слова: *алгоритми машинного навчання (MLA), геостатистичне та ГІС-моделювання, фосфатна руда Абу Тартур*